Science of the Total Environment 953 (2024) 175984

Contents lists available at ScienceDirect

Science of the Total Environment

journal homepage: www.elsevier.com/locate/scitotenv

# Understanding the impact of environmentally relevant alkyl C12-16 dimethylbenzyl ammonium chloride concentrations on zebrafish health

Gustavo Axel Elizalde-Velázquez [a,1], Omar Gómora-Martínez [a,1], Demetrio Raldua [b], Selene Elizabeth Herrera-Vázquez [a], Leobardo Manuel Gómez-Oliván [a,*]

[a] Laboratorio de Toxicología Ambiental, Facultad de Química, Universidad Autónoma del Estado de México, Paseo Colón intersección Paseo Tollocan, Colonia Residencial Colón, CP 50120 Toluca, Estado de México, Mexico
[b] Institute of Environmental Assessment and Water Research (IDAEA-CSIC), Jordi Girona 18, 08034 Barcelona, Spain

## HIGHLIGHTS

- ADBAC C12-C16 instigated an oxidative stress response within zebrafish organs.
- Expression of apoptotic-related genes displayed a notable increase across all organs.
- The gills and gut exhibited the most pronounced effects among the organs studied.
- Realistic concentrations of ADBAC C12-C16 pose a threat to aquatic species.

## GRAPHICAL ABSTRACT

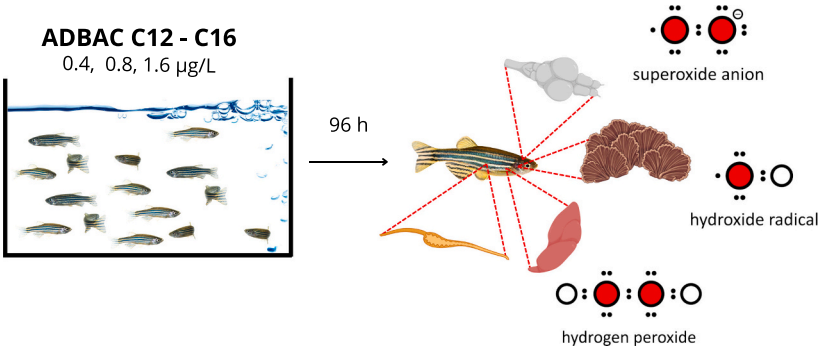


## ARTICLE INFO

Editor: Damia Barcelo

*Keywords:*
Zebrafish
Quaternary ammonium compounds
Oxidative damage
Apoptosis

## ABSTRACT

Alkyldimethylbenzylammonium chlorides (ADBACs), classified as second-generation quaternary ammonium compounds, are extensively employed across various sectors, encompassing veterinary medicine, food production, pharmaceuticals, cosmetics, ophthalmology, and agriculture. Consequently, significant volumes of ADBAC C12-C16 are discharged into the environment, posing a threat to aquatic organisms. Regrettably, comprehensive data regarding the toxicological characteristics of these compounds remain scarce. This research aimed to determine whether or not ADBAC C12-C16, at environmentally relevant concentrations (0.4, 0.8, and 1.6 µg/L), may instigate oxidative stress and alter the expression of apoptosis-related genes in the liver, brain, gut, and gills of *Danio rerio* adults (5–6 months). The findings revealed that ADBAC C12-C16 elicited an oxidative stress response across all examined organs following 96 h of exposure. Nonetheless, the magnitude of this response varied among organs, with the gills exhibiting the highest degree of susceptibility, followed by the gut, liver, and brain, in descending order. Only the gut and gills of the examined organs displayed a concentration-dependent reduction in the activity of superoxide dismutase (SOD) and catalase (CAT). Akin to the oxidative stress response, all organs exhibited a marked increase in *bax*, *blc2*, *casp3*, and *p53* expression levels. However, the gills and gut manifested a distinctive suppression in the expression of *nrf1* and *nrf2*. Our Principal Component Analysis (PCA)

* Corresponding author.
*E-mail address:* lmgomezo@uaemex.mx (L.M. Gómez-Oliván).
[1] These authors contributed equally.

https://doi.org/10.1016/j.scitotenv.2024.175984
Received 21 May 2024; Received in revised form 30 July 2024; Accepted 31 August 2024
Available online 5 September 2024

confirmed that SOD, CAT, nrf1, and nrf2 were negatively correlated to oxidative damage biomarkers and apoptosis-related genes in the gills and gut; meanwhile, in the remaining organs, all biomarkers were extensively correlated. From the above, it can be concluded that ADBAC C12-C16 in low and environmental concentrations may threaten the health of freshwater fish.

## 1. Introduction

Quaternary ammonium compounds, commonly referred to as QACs, represent a prevalent class of cationic surfactants extensively utilized in fabric softeners, antistatic agents, disinfectants, biocides, detergents, phase transfer agents, and various personal care products (Bureš, 2019). Among the second-generation QACs, alkyldimethylbenzylammonium chlorides (ADBACs) stand out, distinguished by possessing an alkyl chain comprising more than eight carbons (ADBAC C8-C18) (Sharma et al., 2022). It is worth noting, however, that within the spectrum of ADBACs, only those featuring alkyl chains of C12-16 are approved by the regulatory framework governing biocidal products across diverse applications, including Type 3 (veterinary hygiene), 4 (food processing areas), and 8 (wood preservatives) products (European Food Safety Authority, 2023). Moreover, recent research has revealed that ADBAC C12-C16 compounds act as antimicrobial preservatives in pharmaceutical, cosmetic, and ophthalmic products while also serving as biocides in agriculture (Gerba, 2015; Carrijo-Carvalho et al., 2017; El-Fawy et al., 2023).

Due to the extensive use of ADBAC in residential and industrial contexts, significant volumes of ADBAC C12-C16 find their way to wastewater treatment facilities. Within these facilities, their elevated affinity for adsorption onto activated sludge impedes their removal, leading to an ongoing release of these compounds into aquatic ecosystems (Clara et al., 2007; Li et al., 2014). Indeed, the primary sources responsible for the environmental release of C12-C16 ADBAC are the effluent discharges and sludge from wastewater treatment plants (WWTPs) (Zhang et al., 2015). However, it has been pointed out by other researchers that localized sources such as hospitals, laundry wastewater, and roof runoff may also contribute to the introduction of C12-C16 ADBAC into water bodies (Van de Voorde et al., 2012; Zhang et al., 2015; Luz et al., 2020). Currently, the concentration ranges of ADBAC C12-C16 are 0.014 to 170 μg/L in influents (Clara et al., 2007; Östman et al., 2017), 0.00092 to 100 μg/L in effluents (Ding and Liao, 2001; Li et al., 2020), 0.009 to 188 mg/kg in activated sludge (Ruan et al., 2014; Heyde et al., 2020), 0.004 to 8.9 mg/kg in sediments (Li and Brownawell, 2010; Pintado-Herrera et al., 2017), and 0.0004 to 255 μg/L in surface water (Ding and Liao, 2001; Olkowska et al., 2013; Kim et al., 2020).

Despite the widespread research on ADBAC C12-C16 entering aquatic environments, there is a paucity of studies examining their detrimental effects on aquatic organisms. To date, four studies have investigated the potential impacts of these compounds on various hydrobiont species (Zhu et al., 2010; Chen et al., 2014; Lavorgna et al., 2016; Christen et al., 2017). In the case of *Chlorella vulgaris*, for instance, Zhu et al. (2010) found that the effective concentration 50 (EC50) of ADBAC C12-C16 ranged from 0.0456 to 0.0576 mg/L after 96 h, while Chen et al. (2014) reported a value of 5.80 mg/L for ADBAC C12 after 48 h. Additionally, Lavorgna et al. (2016) indicated that in *Ceriodaphnia dubia*, the EC50, lowest observed effect concentration (LOEC), and no observed effect concentration (NOEC) of ADBAC C8-C18 were 43.97 μg/L, 4 ng/L, and 0.4 ng/L, respectively. The study conducted by Christen et al. (2017), stands out as the only study to document a dose-dependent elevation in genes associated with oxidative stress, such as *atf-4*, *atf-6*, *xbp-1s*, and *tnf-α*, within *Danio rerio* embryos following 120 h of exposure. As can be seen, the studies are limited by their focus on a few species, variability in reported toxicity values, short exposure durations, and a lack of comprehensive mechanistic insights, reflecting a need for further research to assess the full environmental impact of ADBACs.

Bearing in mind the above, the following inquiries were raised: 1) Can environmentally relevant concentrations of ADBAC C12-C16 (0.4, 0.8, and 1.6 μg/L) induce oxidative stress and apoptosis in the liver, gills, intestines, and brain of *Danio rerio* after? 2) Which organ of the fish will exhibit the most pronounced effects from ADBAC C12-C16 after 96 h of exposure? and 3) What is the underlying mechanism by which ADBAC C12-C16 may induce a harmful response in *Danio rerio*? Considering ADBAC may undergo some oxidative metabolism in the liver (Luz et al., 2020), it is anticipated that ADBAC C12-C16 will induce a toxic response in all organs, with the liver being the most affected.

## 2. Method

### 2.1. Reagents

The ADBAC C12-C16 compound, with a purity exceeding 95 % and designated by the CAS number 68424-85-1, was procured from BIOSYNTH, headquartered in San Diego, California. Furthermore, unless expressly stated otherwise, all additional chemical substances were sourced from Sigma Aldrich, headquartered in St. Louis, Missouri.

### 2.2. Zebrafish husbandry

Adult zebrafish belonging to the AB strain were accommodated at the Autonomous University of Mexico State in 100-liter aquaria. These aquaria upheld a proportional allocation of one zebrafish per liter of water and featured constant aeration. The dechlorinated and UV-filtered water was renewed every three days. Additionally, each aquarium's temperature and light-dark cycle were maintained at 27 °C ± 1 °C and 10-14 h, respectively. The feeding schedule comprised three daily sessions, during which Spirulina flakes sourced from Ocean Nutrition (US) were provided.

### 2.3. Zebrafish exposure

80 adult zebrafish, aged between 5 and 6 months and measuring 3.4 ± 0.1 cm in length and 498 ± 31 mg in weight, were evenly distributed across four batches. Each batch contained 20 fish with an equal ratio of females to males (1:1) housed in 20 l of water treated with dechlorination and UV filtration. Within this setup, one system functioned as the control group while the other three were used to subject adult zebrafish to one of the concentrations employed of C12–C16 ADBAC (0.4, 0.8, and 1.6 μg/L). The concentrations employed in this study are not only deemed environmentally pertinent (Ding and Liao, 2001; Clara et al., 2007; Li and Brownawell, 2010; Olkowska et al., 2013; Ruan et al., 2014; Östman et al., 2017; Li et al., 2020; Heyde et al., 2020) but also have been demonstrated to elicit harmful effects in *Chlorella vulgaris*, *Ceriodaphnia dubia*, and *Danio rerio* (Zhu et al., 2010; Chen et al., 2014; Lavorgna et al., 2016; Christen et al., 2017). The exposure period spanned 96 h, during which a consistent temperature (27 ± 1 °C) and light-dark cycle (14 h:10 h), mirroring the conditions for fish maintenance, were maintained. Based on the research mentioned above, a 96-hour exposure period was chosen, as this duration has been demonstrated to be sufficient for ADBACs to induce a toxic response in zebrafish and other aquatic organisms. The water was renewed every alternate day throughout the experimental duration. The exposure of zebrafish under the above conditions was repeated three times in three independent experiments ($n = 240$).

### 2.4. Zebrafish euthanasia and dissection

After the designated exposure period, no dead fish were observed in either the control group or the batches containing ADBAC C12-C16. Therefore, the twenty fish exposed in each batch were utilized for subsequent analyses, which involved quantifying oxidative stress and assessing gene expression, with ten fish assigned to each assay. Euthanasia was induced by hypothermic shock for all fish. Following euthanasia, A meticulous dissection with dissecting forceps was then carried out to extract the brain, liver, gills, and gut from each fish. The dissected organs were carefully placed into conical microtubes. For oxidative stress quantification, microtubes were filled with 1 mL of phosphate-buffered saline solution (pH of 7.4). In contrast, microtubes designated for gene expression evaluation were filled with RNALater (QIAGEN). These microtubes were conscientiously stored at a controlled temperature ranging from 2 °C to 4 °C until further analysis.

### 2.5. Oxidative stress assessment

The tissue was subjected to homogenization using a rotor-stator homogenizer at 10,000 rpm for 30 s, yielding two tubes for each homogenized sample. In the primary tube, a blend comprising 300 μL of homogenate and an equal volume of 20 % trichloroacetic acid underwent centrifugation at 11495 rpm and 4.0 °C for 15 min. The ensuing precipitate was then employed to quantify carbonylated protein content (PCC), following the methodology delineated by Levine et al. in 1994. Concurrently, the supernatant was utilized to assess the levels of lipoperoxidation (LPX) and hydroperoxides (HPC), adhering to the protocols expounded by Buege and Aust in 1978 and Jiang et al. in 1992, respectively. In the secondary tube, 700 μL of homogenate underwent centrifugation at 12,500 rpm and 4.0 °C for 15 min. The resulting supernatant was employed for the determination of superoxide dismutase (SOD) and catalase, following the procedures outlined by Misra and Fridovich in 1972 and Radi et al. in 1991, respectively. The quantification of all biomarkers' results was standardized utilizing the Bradford method, as detailed by Bradford in 1976.

### 2.6. qPCR

RNA isolation and reverse transcription from each tissue sample were conducted using the RNeasy Mini Kit (QIAGEN) and the QuantiTect Reverse Transcription Kit (QIAGEN). The qPCR was executed utilizing the Gene Q Rotor manufactured by QIAGEN. This involved the application of 25 μL of the 2× QuantiTect SYBR Green PCR solution, in addition to 1.0 μL of each primer (as detailed in Table 1), 4.0 μL of cDNA, and 19 μL of RNase-free water. The thermal cycling program commenced with an initial denaturation phase at 94 °C for 10 min, followed by 35 cycles comprising denaturation at 94 °C for 15 s, primer annealing for 30 s, and extension at 72 °C for 30 s. For normalization of target gene expression levels, the β-actin gene was employed. The selection of target genes was strategically made to elucidate the role of the antioxidant response, mainly mediated by nrf1 and nrf2, in counteracting oxidative damage potentially induced by ADBAC C12-C16. Nrf1 and nrf2 are pivotal in regulating the cellular defense mechanisms against oxidative stress (Ngo and Duennwald, 2022). Therefore, insights into how these transcription factors mediate cellular responses to oxidative insults can be gained by examining their expression. Additionally, the expression of p53, casp3, bax, and bcl2 was analyzed to evaluate the impact of the compound on cellular survival and apoptotic pathways. These genes were chosen due to their critical roles in apoptosis and cellular stress responses: p53 is a crucial regulator of the cell cycle and apoptosis (Wang et al., 2022), casp3 is an executioner caspase essential for apoptosis (Araya et al., 2021), bax promotes apoptosis by inducing mitochondrial outer membrane permeabilization (Kuwana et al., 2020), and bcl2 functions as an anti-apoptotic factor by inhibiting such permeabilization (Qian et al., 2022). Understanding the expression of the genes mentioned above could offer a more comprehensive perspective on how ADBAC C12-C16 induces growth inhibition and mortality in various hydrobiont species (Zhu et al., 2010; Chen et al., 2014; Lavorgna et al., 2016; Christen et al., 2017). After the amplification cycles, an analysis of the dissociation curve was conducted using specific parameters: an initial denaturation phase at 95 °C for 10 s, a reduction to 65 °C for 10 s, and a gradual increment back to 95 °C for 10 s, with increments of 0.2 °C. The above protocol was implemented to discern specific products from non-specific ones within the samples, with data systematically gathered at each increment of the melting curve. To corroborate the findings, negative controls were included, utilizing samples devoid of template, with RNase-free water serving as the alternative. The quantification of alterations in mRNA expression was performed using the $2^{-\Delta\Delta Cq}$ method, following the methodological framework delineated by Pfaffl in 2001, Pfaffl et al. in 2002, and Schmittgen and Livak in 2008.

**Table 1**
Nucleotide sequences of the primers crafted for gene expression analysis utilizing qPCR.

| Gen | Forward, reverse | Primer sequence (5′ → 3′) | Access number |
|---|---|---|---|
| *bax* | F | GGC TAT TTC AAC CAG GGT TCC | AF231015 |
| | R | TGC GAA TCA CCA ATG CTG T | |
| *bcl2* | F | TAC GGG ATG CTG GAG ATG AA | NM_001030253 |
| | R | CCC AGT TCA CTC CGT CTC TA | |
| *p53* | F | GCG GAT TTG CTT TGT GGA TG | NM_001271820 |
| | R | CCG ACC TCC TCT CCA CTA AA | |
| *casp3* | F | GATGAACGGAGACTGTGTGG | NM_131877.3 |
| | R | CTGAAGGCATGGGATTGAGG | |
| *nrf1* | F | CAG TGA CAG TAG CCC AGG TG | NM_001328540.1 |
| | R | CTG ACG CTT GTG TGG TTT GG | |
| *nrf2* | F | GGC GAT CCT CCT GTA AAC CC | NM_182889.1 |
| | R | CCG AAG GAT CCG TCT TCG GT | |

bax: B-cell lymphoma 2 associated X. bcl2: B-cell lymphoma 2. p53: tumor protein p53. casp3:caspase 3. nrf1: nuclear respiratory factor 1. nrf2: nuclear factor erythroid 2-related factor 2.

### 2.7. ADBAC C12-C16 quantification

Water samples of 10 mL were collected at the beginning and after 96 h from each of four different batches. The tissue samples were handled per the protocol by Łabuzek et al. (2010). Initially, *Danio rerio* organs were homogenized and then deproteinized using 400 μL of acetonitrile and 500 μL of methanol, which contained the internal standard at a concentration of 5.7 μmol/L. The homogenate was filtered through a 10 μm sieve and dried at 45 °C under a nitrogen stream. The dried material was dissolved in 100 μL of the mobile phase and centrifuged at 16,000*g* for 15 min. Analysis of both tissues and water samples was conducted with an Agilent 1260 HPLC system paired with an API 5500 Qtrap MS. Chromatographic separation was achieved using an Acclaim Surfactant Plus column (150 × 3.0 mm, 3 μm particle size) from Thermo Scientific, maintained at a temperature of 30 °C. The experiments employed isocratic elution conditions with a 0.5 mL/min flow rate. The mobile phase was a 50:50 (*v*/v) blend of acetonitrile and 0.2 M ammonium acetate solution. Analyst 1.6 software facilitated data acquisition and processing. Calibration was performed using a five-point curve prepared by adding ADBAC C12-C16 to ultrapure water at concentrations between 0.01 μg/L and 5 μg/L.

### 2.8. Statistical analysis

Organs gathered from the three independent experiments were analyzed throughout the abovementioned procedures. Additionally, each organ sample was measured thrice, yielding nine data points for each oxidative stress biomarker and gene. These data points were utilized for statistical scrutiny and were presented in the conventional

format of mean values accompanied by their respective standard deviations (SD). The pandas-profiling library in Python confirmed that all variables were complete and lacked missing data. Homogeneity of variance was confirmed by applying the Bartlett test, while the evaluation of normal distribution was executed utilizing the Shapiro-Wilk test. Differences in means were determined employing the Tukey test, with a significance threshold established at $p < 0.05$. A one-way ANOVA test was administered through Sigma Plot 12.3 software to explore differences among treatment groups, maintaining a significance level of $\alpha = 0.05$. A Principal Component Analysis (PCA) was undertaken to assess the strength of the correlation between oxidative stress and gene expression, with a predetermined significance threshold of $p < 0.05$. The dataset for PCA consisted of 11 numerical variables (*nrf1*, *nrf2*, *p53*, *bax*, *bcl2*, *casp3*, SOD, CAT, LPX, HPC, PCC) and 4 observations (Control, C1, C2, C3). The data were normalized to ensure each variable contributed equally to the analysis. The correlation matrix was computed from the normalized data to capture the relationships between variables. Briefly, the Pearson correlation coefficient between two variables, *Xi* and *Xj*, was calculated using: $Pij = \frac{Cov(Xi,Xj)}{\sigma Xi \bullet \sigma Xj}$, where *Pij* is the correlation coefficient between variables *Xi* and *Xj*, $Cov(Xi, Xj)$ is the covariance between *Xi* and *Xj*, and $\sigma Xi$ and $\sigma Xj$ are the standard deviations of *Xi* and *Xj*. For standardized data, $\sigma Xi$ and $\sigma Xj$ are 1, simplifying the correlation coefficient to the covariance. The covariance between two variables, *Xi* and *Xj*, was calculated as: $Cov(Xi, Xj) = \frac{1}{n-1} \sum_{k=1}^{n} (Xik - \overline{Xi})(Xjk - \overline{Xj})$, where n is the number of observations, and $\overline{Xi}$ and $\overline{Xj}$ are the means of *Xi* and *Xj*. Eigenvectors and eigenvalues were derived from this matrix using spectral decomposition. Concisely, the eigenvalues λ were obtained by solving the characteristic equation: $\det(C - \lambda I) = 0$, where det denotes the determinant of the matrix, C is the correlation matrix, λ represents the eigenvalues, and *I* is the identity matrix. For each eigenvalue λ, the corresponding eigenvector $\upsilon$ was determinate by $(C - \lambda I)\,\upsilon = 0$, where $\upsilon$ is the eigenvector associated with the eigenvalue λ and the matrix $(C - \lambda I)$ is formed by subtracting λ from the diagonal elements of C. Methods such as Gaussian elimination or matrix factorization techniques were employed to find the eigenvectors. These computational procedures were carried out using R's FactoMineR and factoextra packages. Additional support was provided by packages such as Matrix, psych, and stats for various PCA and matrix operations. The number of principal components to retain was determined by examining the percentage of explained variance and the scree plot. The cumulative explained variance was examined to ensure sufficient components were retained to demonstrate at least 90 % of the variance. Likewise, a scree plot was generated to visually inspect the eigenvalues and identify the "elbow" point where the eigenvalues level off, indicating the optimal number of components to retain. The original data were then projected onto the new principal component space using the selected eigenvectors.

## 3. Results

### 3.1. Oxidative stress

In all organs of fish exposed to ADBAC C12-C16, an oxidative stress response was noted, distinguished by either an escalation or diminution in the levels of all oxidative stress biomarkers (Fig. 1 A–D). Notwithstanding, it is imperative to acknowledge that the responses manifested differences across the organs and concentrations. As an illustration, the gills and gastrointestinal tract demonstrated the most significant adverse effects, succeeded by impacts observed in the liver and brain. This observation is substantiated by the evident concentration-dependent inhibition of SOD and CAT in the gills and gut, juxtaposed with the contrasting response observed in the liver and brain. Likewise, the preceding assertion also finds corroboration in the particularly conspicuous elevation of oxidative damage biomarkers in the gills and gastrointestinal tract, noted at the lowest concentration of ADBAC C12-C16. At the middle concentration, it is paramount to note that the liver showed the most substantial increase in LPX, HPC, and PCC, followed by the gills, brain, and gut. The expressions of the nrf1 and nrf2 genes demonstrated a concentration-dependent decrease within the gills and gut, juxtaposed with the contrasting response observed in the liver and brain.

### 3.2. Gene expression

Akin to oxidative stress, the expression of all genes evaluated experienced notable alterations across all fish organs subjected to ADBAC C12-C16, as opposed to those in the control group (Fig. 2). However, these changes in gene expression were particularly conspicuous in the gills and gastrointestinal tract. For example, the color gradients depicted in the heat maps (Fig. 2 A–D) exhibited darker shades, indicative of heightened expression levels, in the gills and gastrointestinal tract when fish were exposed to the ADBAC C12-C16 across nearly all genes, except for *nrf1* and *nrf2*. The expressions of the nrf1 and nrf2 genes demonstrated a concentration-dependent decrease within the gills and gut, juxtaposed with the contrasting response observed in the liver and brain. The genes *bax*, *bcl2*, *casp3*, and *p53* displayed increased expression levels consistently across all organs examined.

### 3.3. ADBAC C12-C16 water and tissue levels

In all systems except for the control, ADBAC C12-C16 concentrations in water decreased, with the control remaining below the limit of quantification. It is important to note that ADBAC C12-C16 concentrations did not decrease by >80 % in any system (C1: 87.5 %, C2: 85.0 %, and C3: 80.63 %). Given that the measured concentrations of ADBAC C12-C16 did not exhibit a reduction >20 % relative to the nominal concentration, all analyses were conducted based on the nominal concentration. In the control group, ADBAC C12-C16 concentrations in all organs were below the limit of quantification. In contrast, fish from the treatment groups exhibited a significant increase in ADBAC C12-C16 concentrations across various organs, as detailed in Table 2. The highest absorption of ADBAC C12-C16 was observed in the gut, followed by the gills, liver, and brain. Additionally, ADBAC C12-C16 concentrations in all organs increased in a concentration-dependent manner. Considering the mean concentrations in organs and the measured concentration in water, the bioconcentration factors (BCF) were C1: 0.043, C2: 0.042, and C3: 0.040. The calculated BCFs indicate that the substance has a low potential for bioconcentration.

### 3.4. PCA

Our PCA aligned with earlier observations, revealing a robust and positive correlation among all the biomarkers assessed in the liver and brain (Fig. 3 A and D). Likewise, it showed that the oxidative damage biomarkers and apoptosis-related genes scrutinized in the gills and gut exhibited consistently strong positive correlations. Moreover, it was observed that p53, bax, bcl2, casp3, LPX, HPC, and PCC exhibited a negative correlation with SOD, CAT, nrf1, and nrf2 within the same organs where the suppression or reduction in the levels of antioxidant enzymes and genes was noted (Fig. 3 B and C). The cosine squared ($cos^2$) values derived from our PCA across all organs consistently exceeded 0.96. This observation confirms that all biomarkers make substantial contributions to the principal component and exhibit high levels of correlation with one another.

## 4. Discussion

Despite the increased use of ADBAC C12-C16 in several industrial sectors and the imminent and continuous discharge of these compounds into the environment, knowledge regarding the toxic profile of ADBAC C12-C16 remains scarce. Considering this knowledge gap, the current study set out to investigate if ADBAC C12-C16, present in concentrations

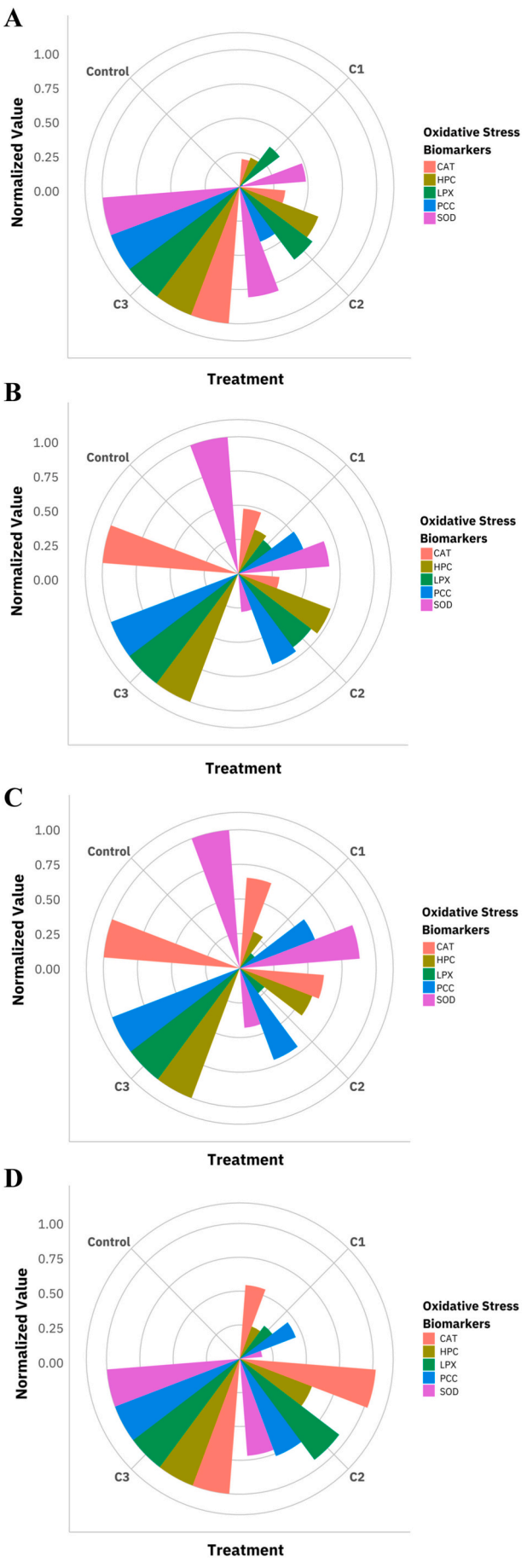


**Fig. 1.** Oxidative stress elicited by ADBAC C12–C16 within the (A) brain, (B) gills, (C) gut, and (D) liver of zebrafish. The presented data depict the mean values ± standard deviation derived from three distinct experiments. Data underwent normalization to facilitate its representation through circular bar charts. Abbreviations: SOD (superoxide dismutase), CAT (catalase), LPX (lipid peroxidation), HPC (hydroperoxide content), PCC (protein carbonyl content), C1: Concentration 1 (0.4 μg/L ADBAC C12–C16), C2: Concentration 2 (0.8 μg/L ADBAC C12–C16), C3: Concentration 3 (1.6 μg/L ADBAC C12–C16).

found in the environment (0.4, 0.8, and 1.6 μg/L), might induce oxidative stress within the liver, brain, intestines, and gills of *Danio rerio*. The findings indicated that ADBAC C12-C16 prompted an oxidative stress response across all examined organs, with the gills displaying the highest degree of susceptibility, followed by the gut, liver, and brain, in descending order. Consistent with these results, a prior study illustrated that *Danio rerio* exposure to ADBAC C12-C14 elicited a concentration-dependent upregulation in the expression of atf-4, atf-6, and xbp-1s, genes implicated in the induction of endoplasmic reticulum (ER) stress (Christen et al., 2017). The endoplasmic reticulum (ER) is the organelle responsible for intricate processes such as protein biosynthesis and post-translational modification processes; however, when cells undergo adverse conditions such as nutrient deprivation, calcium dysregulation, or the accumulation of misfolded proteins, ER stress occurs (Chong et al., 2017). ER stress instigates the unfolded protein response (UPR), a cellular mechanism to reinstate ER equilibrium by curtailing protein synthesis (Hetz, 2012; Read and Schröder, 2021). Unfortunately, should UPR not work, and ER stress persists unabated or escalates, it may prompt oxidative stress. Oxidative stress can also instigate or exacerbate ER stress (Fig. 4). Reactive oxygen species (ROS), comprising highly reactive oxygen-containing molecules, can directly impair ER proteins, fostering the aggregation of misfolded or unfolded proteins and prompting the UPR (Lin et al., 2021). Thus, the interplay between ER stress and oxidative stress manifests as a multifaceted, bidirectional relationship.

For this research's scope, benzalkonium chloride's harmful impacts will be duly examined and discussed. Benzalkonium chloride and ADBACs both belong to the category of QACs. It is noteworthy, however, that while benzalkonium chloride constitutes a blend of ADBACs, ADBACs denote distinct homologs within this mixture (Rogov et al., 2020). Likewise, it is imperative to underscore that although some studies have assessed the toxicological impacts of benzalkonium chloride on aquatic organisms, none have distinctly elucidated the mixture of ADBACs utilized. Considering the preceding, it can be asserted that our findings exhibit certain similarities with those studies employing benzalkonium chloride. As an illustration, prior research employing benzalkonium chloride at concentrations spanning from 0.1 to 2.5 mg/L has demonstrated its capacity to provoke oxidative stress in two different species of fish (Antunes et al., 2016; Sousa et al., 2023). However, differences in oxidative stress response were observed across the studies. In the study conducted by Antunes et al. (2016), for instance, authors reported that CAT activity decreased within the gills and liver tissues of *Oncorhynchus mykiss* after benzalkonium chloride (0.180–1.050 mg/L) exposure. Meanwhile, research conducted by Sousa et al. in 2023 revealed that CAT activity in *Danio rerio* embryos increased at lower concentrations of benzalkonium chloride (0.1 and 0.5 mg/L) and decreased at higher concentrations (2.5 mg/L). Intriguingly, both studies indicated that the biological response to exposure to benzalkonium chloride is dual, contingent upon the exposure concentration. Herein, however, it can be posited that variations in response could stem from inherent disparities among organs, irrespective of the concentrations employed (0.4, 0.8, and 1.6 μg/L). Our PCA substantiates the previously observed hypothesis by indicating a significant positive association between reduced levels of antioxidant-related transcription factors and decreased antioxidant activities of SOD and CAT in the gills and gut. Transcription factors nrf1 and nrf2 are pivotal in cellular

*(caption on next column)*

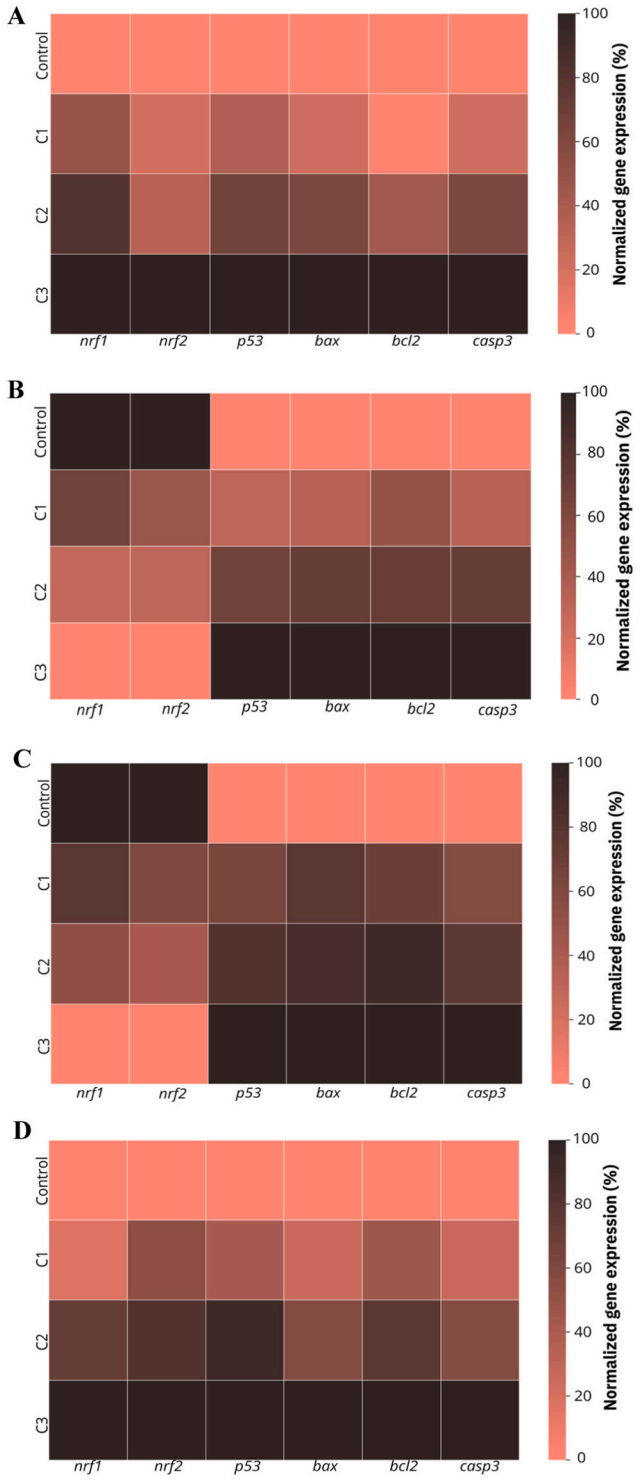


**Fig. 2.** Quantification of gene expression relating to apoptosis regulation (*bax*, *bcl2*, *p53*, and *casp3*) and antioxidant function (*nrf1* and *nrf2*) in zebrafish (A) brain, (B) gills, (C) gut, and (D) liver after exposure to C12–C16 ADBAC. The presented data depict the mean values ± standard deviation derived from three distinct experiments. Data underwent normalization to facilitate its representation through a heat map. The color gradient represents the percentage of normalized gene expression, with orange indicating a low percentage and black indicating a high percentage. Abbreviations: bax (B-cell lymphoma 2 associated X), bcl2 (B-cell lymphoma 2), p53 (tumor protein p53), casp3(caspase 3), nrf1 (nuclear respiratory factor 1), nrf2 (nuclear factor erythroid 2-related factor 2), C1: Concentration 1 (0.4 μg/L ADBAC C12–C16), C2: Concentration 2 (0.8 μg/L ADBAC C12–C16), C3: Concentration 3 (1.6 μg/L ADBAC C12–C16).

**Table 2**
Measured concentrations of ADBAC C12-C16 in water samples and *Danio rerio* tissues.

| Nominal concentration | Measured concentration (μg/L) | |
|---|---|---|
| | 0 hpf | 96 hpf |
| Water samples | | |
| Control (0 μg/L) | <LOD | <LOD |
| C1 | 0.43 ± 0.02 | 0.35 ± 0.03 |
| C2 | 0.79 ± 0.05 | 0.68 ± 0.04 |
| C3 | 1.61 ± 0.03 | 1.29 ± 0.06 |
| Brain samples | | |
| Control (0 μg/L) | <LOD | <LOD |
| C1 | N.A | 0.009 ± 0.003 |
| C2 | N.A | 0.017 ± 0.008 |
| C3 | N.A | 0.048 ± 0.001 |
| Gills samples | | |
| Control (0 μg/L) | <LOD | <LOD |
| C1 | N.A | 0.017 ± 0.002 |
| C2 | N.A | 0.033 ± 0.006 |
| C3 | N.A | 0.051 ± 0.005 |
| Gut samples | | |
| Control (0 μg/L) | <LOD | <LOD |
| C1 | N.A | 0.023 ± 0.005 |
| C2 | N.A | 0.045 ± 0.001 |
| C3 | N.A | 0.071 ± 0.006 |
| Liver samples | | |
| Control (0 μg/L) | <LOD | <LOD |
| C1 (0.4 μg/L) | N.A | 0.011 ± 0.004 |
| C2 (0.8 μg/L) | N.A | 0.020 ± 0.009 |
| C3 (1.6 μg/L) | N.A | 0.033 ± 0.002 |

The presented data depict the mean values ± standard deviation derived from three distinct experiments. Limit of detection: 0.001 μg/L. Abbreviations: <LOD (below limit of detection), N.A: (not analyzed), C1: Concentration 1 (0.4 μg/L ADBAC C12–C16), C2: Concentration 2 (0.8 μg/L ADBAC C12–C16), C3: Concentration 3 (1.6 μg/L ADBAC C12–C16).

defense against oxidative stress and regulating antioxidant response elements (AREs) (Sekine and Motohashi, 2024). Under oxidative, endoplasmic reticulum stress, or phosphorylation through various kinases such as 5′ adenosine monophosphate-activated protein kinase (AMPK) (Elizalde-Velázquez et al., 2022), nrf1 and nrf2 undergo cleavage, translocate to the nucleus, dimerize with small Maf proteins, and bind to AREs in the promoter regions of target genes, thereby facilitating their transcriptional activation (Otsuki and Yamamoto, 2020; Katsuoka et al., 2022). This mechanism typically promotes the expression of SOD and CAT genes in response to oxidative stress (Fig. 4). Nonetheless, in the presence of ADBACs C12-C16, the upregulation of these genes proves insufficient to counterbalance the increased oxidative damage, leading to substantial oxidative stress in the gill and intestinal tissues. This interpretation is further validated by the positive correlations observed between biomarkers of oxidative damage and genes related to apoptosis, underscoring a cohesive response to oxidative stress. Likewise, consistent with our findings, a recent study by Kwon et al. (2020) demonstrated that exposure to benzalkonium chloride at concentrations of 0.05, 0.1, and 0.2 mg/L resulted in the upregulation of several stress response proteins, including superoxide dismutase (SOD), peroxiredoxin 6, and glutathione S-transferase in *Oryzias latipes*.

While the precise toxicity mechanism for ADBACs remains unknown, research has suggested that their amphiphilic nature enables interaction with cell membranes via ionic and hydrophobic interactions, resulting in membrane disruption and heightened permeability (Fig. 4) (Antunes et al., 2016; Rogov et al., 2020). Likewise, two more recent studies indicated that mitochondrial dysfunction may be the primary causative

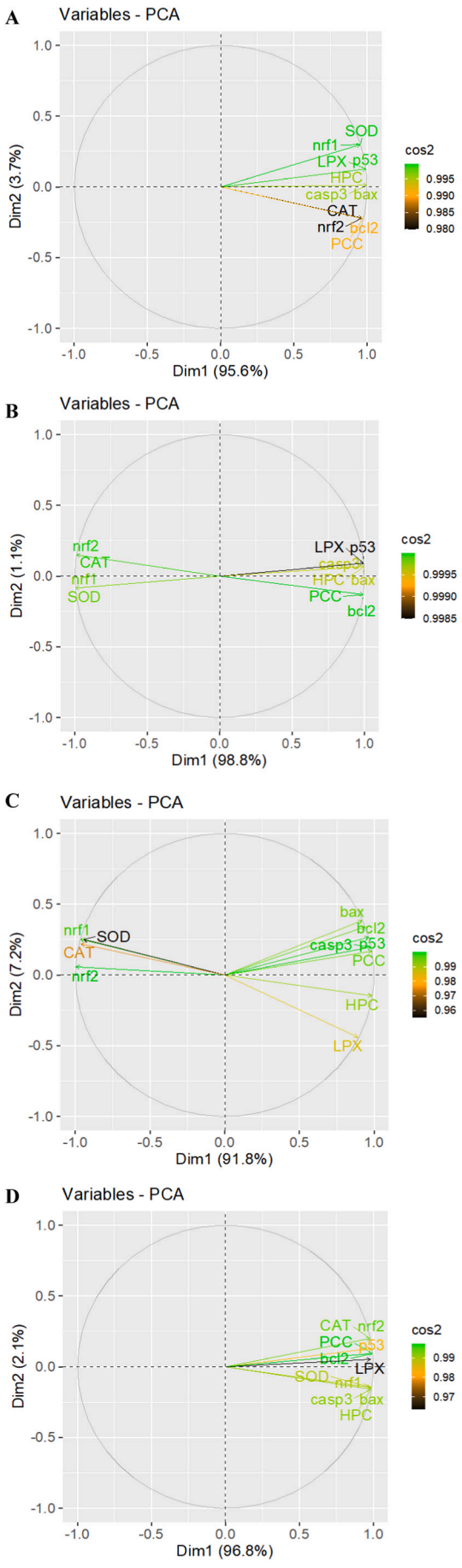


**Fig. 3.** Principal Component Analysis (PCA) of oxidative stress and gene expression data in zebrafish (A) brain, (B) gills, (C) gut, and (D) liver exposed to ADBAC C12-C16. Data underwent normalization to ensure each variable contributed equally to the analysis. The biplots illustrate the distribution and contribution of each biomarker to the principal components. The color gradient represents the contribution of each variable to the principal components, with black indicating low contribution and green indicating high contribution. Abbreviations: SOD (superoxide dismutase), CAT (catalase), LPX (lipid peroxidation), HPC (hydroperoxide content), PCC (protein carbonyl content), bax (B-cell lymphoma 2 associated X), bcl2 (B-cell lymphoma 2), p53 (tumor protein p53), casp3(caspase 3), nrf1 (nuclear respiratory factor 1), nrf2 (nuclear factor erythroid 2-related factor 2), C1: Concentration 1 (0.4 μg/L ADBAC C12–C16), C2: Concentration 2 (0.8 μg/L ADBAC C12–C16), C3: Concentration 3 (1.6 μg/L ADBAC C12–C16).

factor for the adverse effects associated with benzalkonium chloride toxicity (Fig. 4). In the first of these studies, it was documented that benzalkonium chloride hindered mitochondrial adenosine triphosphate (ATP) synthesis and oxygen utilization through a direct interaction with mitochondrial complex I (Datta et al., 2017). Conversely, in the second study, the authors pinpointed that benzalkonium chloride prompted mitochondrial dysfunction, inhibiting respiration during state 3, reducing membrane potential, enabling the opening of the mitochondrial permeability transition pore, enhancing hydrogen peroxide production by mitochondria, and stopping the synthesis of ATP (Rogov et al., 2020). Irrespective of the specific mechanism involved, all pathways lead to the same outcome, namely oxidative damage. Oxidative damage to macromolecules, including DNA, can lead to base modifications, strand breaks, and cross-linking (Fig. 4). When such damage exceeds the cell's repair capabilities, it may result in mutations, genomic instability, and, ultimately cell death through apoptosis or necrosis. The genotoxic effects of benzalkonium chloride, mediated by reactive oxygen species (ROS), have been previously investigated. For example, Antunes et al. (2016) demonstrated that chronic exposure of *Oncorhynchus mykiss* to benzalkonium chloride at concentrations of 0.180 to 1.050 mg/L resulted in significant genotoxic effects. The authors further elucidated that the genotoxic damage caused by benzalkonium chloride involves oxidative assaults on DNA by both reactive oxygen and nitrogen species (ROS/RNS). Additionally, they noted that the DNA damage responses that regulate benzalkonium chloride-induced mutagenesis, such as cell cycle arrest, proliferation, and apoptosis, remain poorly understood. The gene expression of apoptosis-related genes was evaluated in this study to address this knowledge gap. Overall, our findings illustrated that ADBACs C12-C16 elevated bax, bcl2, p53, and casp3 expression levels. These results agreed bax and bcl2 belong to the B-cell lymphoma 2 protein family and are crucial intrinsic or mitochondrial apoptotic pathway regulators. bax promotes apoptosis by forming pores in the mitochondrial membrane, thus releasing pro-apoptotic factors such as cytochrome *c* into the cytoplasm (Dewson and Kluck, 2009; Kuwana et al., 2020). Conversely, bcl2 antagonizes this process by impeding the formation of pores mediated by bax, thereby exerting an anti-apoptotic influence (Qian et al., 2022). The equilibrium between bax and bcl2 levels determines the susceptibility of cells to apoptotic stimuli. p53, a tumor suppressor protein, is a pivotal controller in cellular responses to various stress cues. Upon activation, p53 orchestrates the expression of many target genes involved in cell cycle arrest, DNA repair, senescence, and apoptosis, contingent upon the severity and nature of the cellular stress (Chen, 2016; Wang et al., 2022). Concerning apoptosis, p53 can prompt apoptosis by transcriptionally activating pro-apoptotic genes such as bax (Li, 2021). casp3 serves as a critical executioner caspase, centrally positioned in executing apoptosis. casp3 becomes activated downstream of both the intrinsic and extrinsic apoptotic pathways, culminating in the cleavage of diverse cellular substrates, inclusive of structural and signaling proteins, thereby instigating the characteristic morphological and biochemical alterations associated with apoptosis, such as chromatin condensation, DNA

*(caption on next column)*

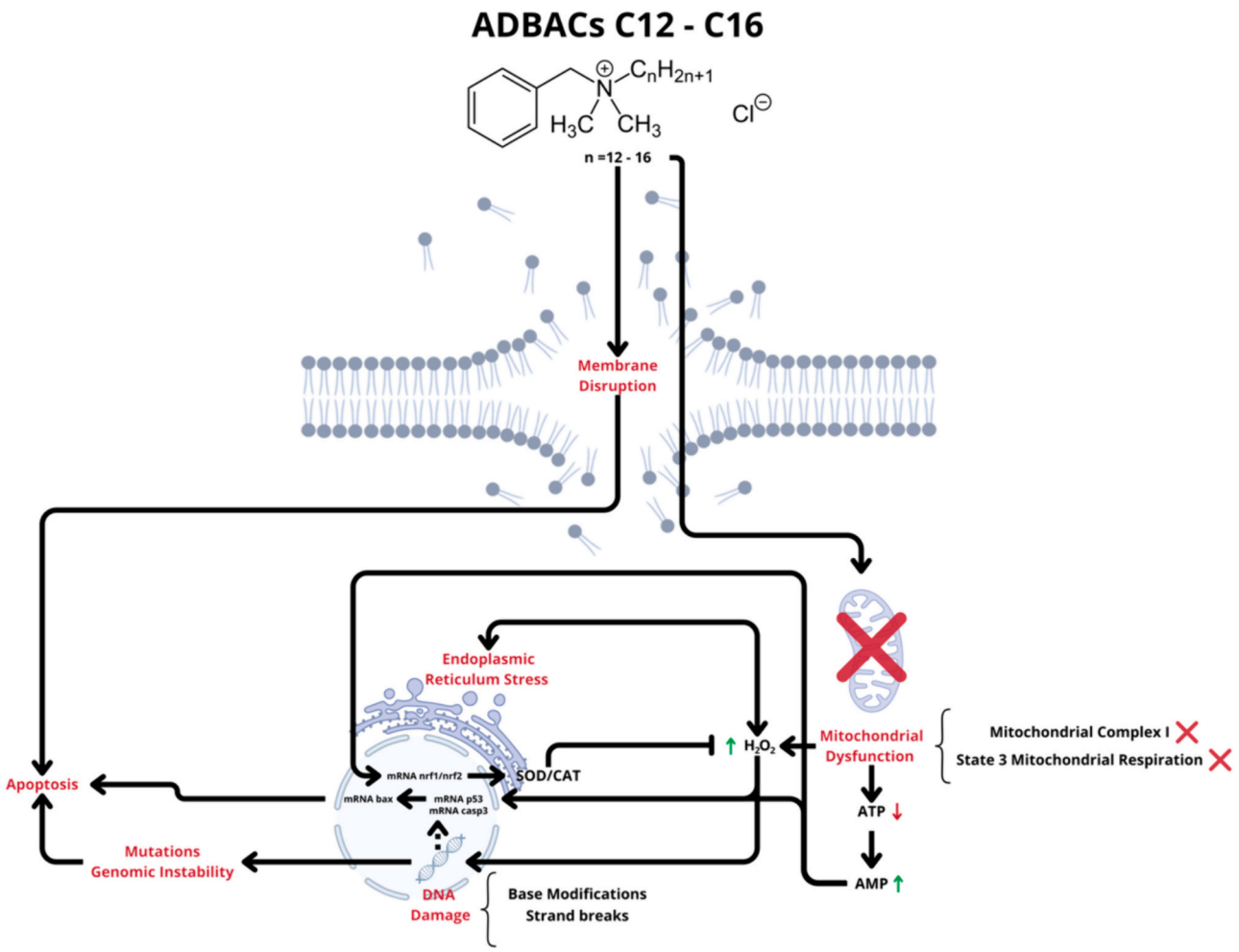


**Fig. 4.** Potential toxicity mechanism by which ADBACs C12 – C16 generate oxidative stress and programmed cell death in hydrobionts. The amphiphilic characteristics of alkyl dimethyl benzyl ammonium chlorides (ADBACs) C12 to C16 enable their interaction with cellular membranes, resulting in membrane disruption and subsequent induction of programmed cell death (apoptosis). Furthermore, ADBACs (C12 – C16) can penetrate cellular membranes, disrupting mitochondrial homeostasis by inhibiting mitochondrial complex I and impairing mitochondrial respiration during state 3. This disruption increases reactive oxygen species (ROS) production, diminished ATP levels, and elevated AMP levels. The overproduction of AMP can activate the AMP-activated protein kinase (AMPK) pathway, which subsequently stimulates transcription factors such as nuclear respiratory and erythroid factors 1 and 2 (nrf1 and 2) that mitigate ROS overproduction through the synthesis of superoxide dismutase (SOD) and catalase (CAT). Likewise, p53 is activated by the AMPK pathway, which in turn activates the pro-apoptotic protein bax and induces apoptosis. Concurrently, elevated ROS levels may trigger endoplasmic reticulum stress, DNA damage, and the activation of apoptosis-related transcription factors, including caspase-3 (casp3), p53, and bax. ROS-induced DNA damage may result in base modifications, strand breaks, and cross-linking. If the extent of this damage surpasses the cell's repair mechanisms, it can lead to mutations, genomic instability, and, ultimately, cell death via apoptosis. Cross-outs denote an inhibition. Green arrows denote an increase. Red arrows denote a decrease. Black arrows denote the direction.

fragmentation, and cellular shrinkage (Araya et al., 2021; Green, 2022). To date, two research endeavors have shown that benzalkonium chloride instigates apoptosis by triggering either casp3 or the proteins bax, bcl2, and p53. Nevertheless, both inquiries were confined to examining human lung epithelial cells exclusively (Kanno et al., 2020; Kim et al., 2020). Hence, this study represents the initial endeavor to elucidate the mechanism by which ADBACs prompt apoptosis across different organs in fish. Fig. 4 depicts and summarizes the potential toxicity mechanisms by which ADBACs C12 – C16 generate oxidative stress and programmed cell death in hydrobionts.

A consensus among researchers is the limited number of studies addressing the toxicity of ADBACs and benzalkonium chloride (Antunes et al., 2016; Sreevidya et al., 2018; Fuchsman et al., 2022). As an illustration, to our current understanding, research on the oxidative damage and genotoxic effects of ADBACs and benzalkonium chloride in aquatic organisms is limited to one study on ADBACs and four studies on benzalkonium chloride. While there are more studies concerning benzethonium chloride, another quaternary ammonium salt, significant structural differences exist between this compound and those studied herein. This scarcity is noteworthy not just because it hinders our ability to compare our findings but also because earlier research suggests that benzalkonium chloride is more toxic than other antimicrobials like triclosan (TCS) and triclocarban (TCC). Sreevidya et al. (2018) conducted experiments to evaluate the detrimental impacts of TCS, TCC, and benzalkonium chloride on two species, *Caenorhabditis elegans* and *Danio rerio*. According to the authors, benzalkonium chloride demonstrated the most significant toxicity among the three compounds, causing acute lethal effects at environmentally relevant concentrations. In light of the aforementioned points, our study is significant for two reasons. Firstly, it addresses the existing knowledge gap concerning the harmful effects of second-generation quaternary ammonium compounds. Secondly, the concentrations utilized in our research are realistic and reflective of those found in environmental settings. However, our study had some limitations that must be considered in future research. For example, the toxic effects of individual ADBACs need to be elucidated (ADBAC C12, ADBAC C14, and ADBAC C16). Thus far, research endeavors, including

our own, have assessed the toxicological implications of the ADBAC blend, with a limited exploration of specific constituents such as ADBAC C12. Conducting focused studies on individual ADBACs is crucial for identifying those with greater toxicity profiles, thereby informing regulatory measures concerning their usage and disposal.

## 5. Conclusions

The QAC ADBAC C12-C16 elicited a noteworthy toxic reaction in the liver, gills, gastrointestinal tract, and brain of *Danio rerio*. Notably, the gills and gastrointestinal tract exhibited the most pronounced deleterious effects, evidenced by a concentration-dependent decrease in antioxidant enzymes. Even though the precise mechanism of toxicity induced by ADBACs remains incompletely understood, three potential pathways have been identified through which this process may occur: disruption of cell membranes, dysfunction of mitochondria, and inhibition of mitochondrial ATP synthesis. Nevertheless, further research is needed to determine whether or not other pathways may be implicated in the toxic response induced by these QACs. Likewise, it is recommended that authors make more significant endeavors to conduct studies utilizing concentrations within the range of ng/L to μg/L. This suggestion is prompted by the observation that concentrations of ADBACs in surface water have been documented to reach levels up to 255 μg/L (Olkowska et al., 2013), and the LOEC in certain aquatic organisms are below 220 ng/L.

## CRediT authorship contribution statement

**Gustavo Axel Elizalde-Velázquez:** Writing – original draft, Formal analysis, Data curation, Conceptualization. **Omar Gómora-Martínez:** Writing – original draft, Investigation, Formal analysis, Data curation, Conceptualization. **Demetrio Raldua:** Writing – review & editing, Visualization, Validation, Supervision, Software, Resources, Investigation, Data curation, Conceptualization. **Selene Elizabeth Herrera-Vázquez:** Writing – original draft, Methodology, Investigation. **Leobardo Manuel Gómez-Oliván:** Writing – review & editing, Writing – original draft, Visualization, Validation, Supervision, Project administration, Funding acquisition, Formal analysis, Data curation, Conceptualization.

## Declaration of competing interest

The authors do not declare any conflicts of interest.

## Data availability

Data will be made available on request.

## Acknowledgments

This study was made possible by financial support the Consejo Nacional de Ciencia y Tecnología (CONACyt, Project 300727).

## References

Antunes, S.C., Nunes, B., Rodrigues, S., Nunes, R., Fernandes, J., Correia, A.T., 2016 Jul. Effects of chronic exposure to benzalkonium chloride in Oncorhynchus mykiss: cholinergic neurotoxicity, oxidative stress, peroxidative damage and genotoxicity. Environ. Toxicol. Pharmacol. 45, 115–122. https://doi.org/10.1016/j.etap.2016.04.016 (Epub 2016 May 13. PMID: 27280532).

Araya, L.E., Soni, I.V., Hardy, J.A., Julien, O., 2021. Deorphanizing caspase-3 and caspase-9 substrates in and out of apoptosis with deep substrate profiling. ACS Chem. Biol. 16 (11), 2280–2296.

Buege, J.A., Aust, S.D., 1978. Microsomal lipid peroxidation. Methods Enzymol. 52, 302–310.

Bureš, F., 2019. Quaternary ammonium compounds: simple in structure, complex in application. Top. Curr. Chem. 377 (3), 14.

Carrijo-Carvalho, L.C., Sant'ana, V.P., Foronda, A.S., de Freitas, D., de Souza Carvalho, F. R., 2017. Therapeutic agents and biocides for ocular infections by free-living amoebae of Acanthamoeba genus. Surv. Ophthalmol. 62 (2), 203–218.

Chen, J., 2016. The cell-cycle arrest and apoptotic functions of p53 in tumor initiation and progression. Cold Spring Harb. Perspect. Med. 6 (3), a026104.

Chen, Y., Geurts, M., Sjollema, S.B., Kramer, N.I., Hermens, J.L., Droge, S.T., 2014. Acute toxicity of the cationic surfactant C12-benzalkonium in different bioassays: how test design affects bioavailability and effect concentrations. Environ. Toxicol. Chem. 33 (3), 606–615.

Chong, W.C., Shastri, M.D., Eri, R., 2017. Endoplasmic reticulum stress and oxidative stress: a vicious Nexus implicated in bowel disease pathophysiology. Int. J. Mol. Sci. 18 (4), 771. https://doi.org/10.3390/ijms18040771. PMID: 28379196; PMCID: PMC5412355. Apr 5.

Christen, V., Faltermann, S., Brun, N.R., Kunz, P.Y., Fent, K., 2017. Cytotoxicity and molecular effects of biocidal disinfectants (quaternary ammonia, glutaraldehyde, poly (hexamethylene biguanide) hydrochloride PHMB) and their mixtures in vitro and in zebrafish eleuthero-embryos. Sci. Total Environ. 586, 1204–1218.

Clara, M., Scharf, S., Scheffknecht, C., Gans, O., 2007. Occurrence of selected surfactants in untreated and treated sewage. Water Res. 41 (19), 4339–4348.

Datta, S., Baudouin, C., Brignole-Baudouin, F., Denoyer, A., Cortopassi, G.A., 2017. The eye drop preservative benzalkonium chloride potently induces mitochondrial dysfunction and preferentially affects LHON mutant cells. Invest. Ophthalmol. Vis. Sci. 58 (4), 2406–2412.

Dewson, G., Kluck, R.M., 2009. Mechanisms by which Bak and Bax permeabilise mitochondria during apoptosis. J. Cell Sci. 122 (16), 2801–2808.

Ding, W.H., Liao, Y.H., 2001. Determination of alkylbenzyldimethylammonium chlorides in river water and sewage effluent by solid-phase extraction and gas chromatography/mass spectrometry. Anal. Chem. 73 (1), 36–40.

El-Fawy, M.M., Abo-Elyousr, K.A., Ahmed, S.A., Korrat, R.A., Saeed, A.S., 2023. Efficacy of N-alkyl dimethyl benzyl ammonium chloride and Bacillus subtilis for control of Cercospora leaf spot disease of sugar beet: in vitro and in vivo studies. Gesunde Pflanzen 75 (6), 2247–2256.

Elizalde-Velázquez, G.A., Gómez-Oliván, L.M., Rosales-Pérez, K.E., Orozco-Hernández, J. M., García-Medina, S., Islas-Flores, H., Galar-Martínez, M., 2022. Chronic exposure to environmentally relevant concentrations of guanylurea induces neurotoxicity of Danio rerio adults. Sci. Total Environ. 819, 153095.

European Food Safety Authority (EFSA), 2023. Risk assessment related to the presence of benzalkonium chloride (BAC), didecyldimethyl ammonium chloride (DDAC) and chlorates in fish and fish products. EFSA J. 21 (5), e08019.

Fuchsman, P., Fetters, K., O'Connor, A., Bock, M., Henning, M., Brown, L., Stanton, K., 2022. Ecological risk analysis for benzalkonium chloride, benzethonium chloride, and chloroxylenol in US disinfecting and sanitizing products. Environ. Toxicol. Chem. 41 (12), 3095–3115.

Gerba, C.P., 2015. Quaternary ammonium biocides: efficacy in application. Appl. Environ. Microbiol. 81 (2), 464–469.

Green, D.R., 2022. Caspases and their substrates. Cold Spring Harb. Perspect. Biol. 14 (3), a041012.

Hetz, C., 2012. The unfolded protein response: controlling cell fate decisions under ER stress and beyond. Nat. Rev. Mol. Cell Biol. 13, 89–102.

Heyde, B.J., Barthel, A., Siemens, J., Mulder, I., 2020. A fast and robust method for the extraction and analysis of quaternary alkyl ammonium compounds from soil and sewage sludge. PloS One 15 (8), e0237020.

Jiang, Z.Y., Hunt, J.V., Wolff, S.P., 1992. Ferrous ion oxidation in the presence of xylenol orange for detection of lipid hydroperoxide in low density lipoprotein. Anal. Biochem. 202, 384–389.

Kanno, S., Hirano, S., Kato, H., Fukuta, M., Mukai, T., Aoki, Y., 2020. Benzalkonium chloride and cetylpyridinium chloride induce apoptosis in human lung epithelial cells and alter surface activity of pulmonary surfactant monolayers. Chem. Biol. Interact. 317, 108962. https://doi.org/10.1016/j.cbi.2020.108962. Feb 1. (Epub 2020 Jan 24. PMID: 31982400).

Katsuoka, F., Otsuki, A., Hatanaka, N., Okuyama, H., Yamamoto, M., 2022. Target gene diversity of the Nrf1-MafG transcription factor revealed by a tethered heterodimer. Mol. Cell. Biol. 42 (3) https://doi.org/10.1128/mcb.00520-21.

Kim, S.H., Kwon, D., Lee, S., Son, S.W., Kwon, J.T., Kim, P.J., Lee, Y.H., Jung, Y.S., 2020. Concentration- and time-dependent effects of benzalkonium chloride in human lung epithelial cells: necrosis, apoptosis, or epithelial mesenchymal transition. Toxics 8 (1), 17. https://doi.org/10.3390/toxics8010017. PMID: 32121658; PMCID: PMC7151738. Mar 2.

Kuwana, T., King, L.E., Cosentino, K., Suess, J., Garcia-Saez, A.J., Gilmore, A.P., Newmeyer, D.D., 2020. Mitochondrial residence of the apoptosis inducer BAX is more important than BAX oligomerization in promoting membrane permeabilization. J. Biol. Chem. 295 (6), 1623–1636.

Kwon, Y.S., Jung, J.W., Kim, Y.J., Park, C.B., Shon, J.C., Kim, J.H., Seo, J.S., 2020. Proteomic analysis of whole-body responses in medaka (Oryzias latipes) exposed to benzalkonium chloride. J. Environ. Sci. Health A 55 (12), 1387–1397.

Łabuzek, K., Suchy, D., Gabryel, B., Bielecka, A., Liber, S., Okopień, B., 2010. Quantification of metformin by the HPLC method in brain regions, cerebrospinal fluid and plasma of rats treated with lipopolysaccharide. Pharmacol. Rep. 62 (5), 956–965.

Lavorgna, M., Russo, C., D'Abrosca, B., Parrella, A., Isidori, M., 2016. Toxicity and genotoxicity of the quaternary ammonium compound benzalkonium chloride (BAC) using Daphnia magna and Ceriodaphnia dubia as model systems. Environ. Pollut. 210, 34–39.

Levine, R.L., Williams, J.A., Stadtman, E.R., Shacter, E., 1994. Carbonyl assays for determination of oxidatively modified proteins. Methods Enzymol. 233, 346–357.

Li, M., 2021. The role of P53 up-regulated modulator of apoptosis (PUMA) in ovarian development, cardiovascular and neurodegenerative diseases. Apoptosis 26 (5), 235–247.
Li, X., Brownawell, B.J., 2010. Quaternary ammonium compounds in urban estuarine sediment environments-a class of contaminants in need of increased attention? Environ. Sci. Technol. 44 (19), 7561–7568.
Li, X., Luo, X., Mai, B., Liu, J., Chen, L., Lin, S., 2014. Occurrence of quaternary ammonium compounds (QACs) and their application as a tracer for sewage derived pollution in urban estuarine sediments. Environ. Pollut. 185, 127–133.
Li, W.L., Zhang, Z.F., Sparham, C., Li, Y.F., 2020. Validation of sampling techniques and SPE-UPLC/MS/MS for home and personal care chemicals in the Songhua Catchment, Northeast China. Sci. Total Environ. 707, 136038.
Lin, H., Peng, Y., Li, J., Wang, Z., Chen, S., Qing, X., Pu, F., Lei, M., Shao, Z., 2021. Reactive oxygen species regulate endoplasmic reticulum stress and ER-mitochondrial $Ca^{2+}$ crosstalk to promote programmed necrosis of rat nucleus pulposus cells under compression. Oxid. Med. Cell. Longev. 2021, 8810698. https://doi.org/10.1155/2021/8810698. PMID: 33815661; PMCID: PMC7987452. Mar 16.
Luz, A., DeLeo, P., Pechacek, N., Freemantle, M., 2020. Human health hazard assessment of quaternary ammonium compounds: Didecyl dimethyl ammonium chloride and alkyl (C12–C16) dimethyl benzyl ammonium chloride. Regul. Toxicol. Pharmacol. 116, 104717.
Misra, H.P., Fridovich, I., 1972. The role of superoxide anion in the autoxidation of epinephrine and a simple assay for superoxide dismutase. J. Biol. Chem. 247, 3170–3175.
Ngo, V., Duennwald, M.L., 2022. Nrf2 and oxidative stress: a general overview of mechanisms and implications in human disease. Antioxidants 11 (12), 2345.
Olkowska, E., Polkowska, Ż., Namieśnik, J., 2013. A solid phase extraction–ion chromatography with conductivity detection procedure for determining cationic surfactants in surface water samples. Talanta 116, 210–216.
Östman, M., Lindberg, R.H., Fick, J., Björn, E., Tysklind, M., 2017. Screening of biocides, metals and antibiotics in Swedish sewage sludge and wastewater. Water Res. 115, 318–328.
Otsuki, A., Yamamoto, M., 2020. Cis-element architecture of Nrf2–sMaf heterodimer binding sites and its relation to diseases. Arch. Pharm. Res. 43 (3), 275–285.
Pfaffl, M.W., 2001. A new mathematical model for relative quantification in real-time RT–PCR. Nucleic Acids Res. 29 (9), e45.
Pfaffl, M.W., Horgan, G.W., Dempfle, L., 2002. Relative expression software tool (REST©) for group-wise comparison and statistical analysis of relative expression results in real-time PCR. Nucleic Acids Res. 30 (9), e36.
Pintado-Herrera, M.G., Wang, C., Lu, J., Chang, Y.P., Chen, W., Li, X., Lara-Martín, P.A., 2017. Distribution, mass inventories, and ecological risk assessment of legacy and emerging contaminants in sediments from the Pearl River Estuary in China. J. Hazard. Mater. 323, 128–138.
Qian, S., Wei, Z., Yang, W., Huang, J., Yang, Y., Wang, J., 2022. The role of BCL-2 family proteins in regulating apoptosis and cancer therapy. Front. Oncol. 12, 985363.
Radi, R., Turrens, J.F., Chang, L.Y., Bush, K.M., Carpo, J.D., Freeman, B.A., 1991. Detection of catalase in rat heart mitochondria. J. Biol. Chem. 266, 22028–22034.
Read, A., Schröder, M., 2021. The unfolded protein response: an overview. Biology (Basel) 10 (5), 384. https://doi.org/10.3390/biology10050384. Apr 29. (PMID: 33946669; PMCID: PMC8146082).
Rogov, A.G., Goleva, T.N., Sukhanova, E.I., Epremyan, K.K., Trendeleva, T.A., Ovchenkova, A.P., Aliverdieva, D.A., Zvyagilskaya, R.A., 2020. Mitochondrial dysfunctions may be one of the major causative factors underlying detrimental effects of Benzalkonium chloride. Oxid. Med. Cell. Longev. 2020, 8956504. https://doi.org/10.1155/2020/8956504. Feb 10. (PMID: 32104543; PMCID: PMC7035552).
Ruan, T., Song, S., Wang, T., Liu, R., Lin, Y., Jiang, G., 2014. Identification and composition of emerging quaternary ammonium compounds in municipal sewage sludge in China. Environ. Sci. Technol. 48 (8), 4289–4297.
Schmittgen, T.D., Livak, K.J., 2008. Analyzing real-time PCR data by the comparative CT method. Nat. Protoc. 3 (6), 1101–1108.
Sekine, H., Motohashi, H., 2024. Unique and overlapping roles of NRF2 and NRF1 in transcriptional regulation. J. Clin. Biochem. Nutr. 74 (2), 91.
Sharma, A., Singh, N., Thomas, A., Srivastava, P., Sharma, A., 2022. Quaternary ammonium compounds: usage in households during COVID-19 pandemic, boon or bane. Asian Pacific J Health Sc 9, 133–139.
Sousa, B., Domingues, I., Nunes, B., 2023 Sep. A fish perspective on SARS-CoV-2: toxicity of benzalkonium chloride on Danio rerio. Environ. Toxicol. Pharmacol. 102, 104200. https://doi.org/10.1016/j.etap.2023.104200 (Epub 2023 Jun 30. PMID: 37394081).
Sreevidya, V.S., Lenz, K.A., Svoboda, K.R., Ma, H., 2018. Benzalkonium chloride, benzethonium chloride, and chloroxylenol-three replacement antimicrobials are more toxic than triclosan and triclocarban in two model organisms. Environ. Pollut. 235, 814–824.
Van de Voorde, A., Lorgeoux, C., Gromaire, M.C., Chebbo, G., 2012. Analysis of quaternary ammonium compounds in urban stormwater samples. Environ. Pollut. 164, 150–157.
Wang, Y.H., Ho, T.L., Hariharan, A., Goh, H.C., Wong, Y.L., Verkaik, N.S., Lane, D.P., 2022. Rapid recruitment of p53 to DNA damage sites directs DNA repair choice and integrity. Proc. Natl. Acad. Sci. 119 (10), e2113233119.
Zhang, C., Cui, F., Zeng, G.M., Jiang, M., Yang, Z.Z., Yu, Z.G., Shen, L.Q., 2015. Quaternary ammonium compounds (QACs): a review on occurrence, fate and toxicity in the environment. Sci. Total Environ. 518, 352–362.
Zhu, M., Ge, F., Zhu, R., Wang, X., Zheng, X., 2010. A DFT-based QSAR study of the toxicity of quaternary ammonium compounds on Chlorella vulgaris. Chemosphere 80 (1), 46–52.